

OXYGEN TRANSPORT IN THE $\text{Sr}_2\text{Fe}_{3-x}\text{Co}_x\text{O}_y$ SYSTEM*

B. Ma and U. Balachandran
Energy Technology Division, Argonne National Laboratory
Argonne, IL 60439

B. J. Mitchell and J. W. Richardson, Jr.
Intense Pulsed Neutron Source, Argonne National Laboratory
Argonne, IL 60439

J. P. Hodges and J. D. Jorgensen
Materials Science Division, Argonne National Laboratory
Argonne, IL 60439

November 1998

The submitted manuscript has been created by the University of Chicago as Operator of Argonne National Laboratory ("Argonne") under Contract No. W-31-109-ENG-38 with the U.S. Department of Energy. The U.S. Government retains for itself, and others acting on its behalf, a paid-up, nonexclusive, irrevocable worldwide license in said article to reproduce, prepare derivative works, distribute copies to the public, and perform publicly and display publicly, by or on behalf of the Government.

Paper for submittal to the Materials Research Society 1998 Fall Meeting,
Nov. 30 - Dec. 4, Boston, 1998.

*Work at Argonne National Laboratory is supported by U.S. Department of Energy, Federal Energy Technology Center, under Contract W-31-109-Eng-38.

RECEIVED
SEP 28 1998
STI

DISCLAIMER

This report was prepared as an account of work sponsored by an agency of the United States Government. Neither the United States Government nor any agency thereof, nor any of their employees, make any warranty, express or implied, or assumes any legal liability or responsibility for the accuracy, completeness, or usefulness of any information, apparatus, product, or process disclosed, or represents that its use would not infringe privately owned rights. Reference herein to any specific commercial product, process, or service by trade name, trademark, manufacturer, or otherwise does not necessarily constitute or imply its endorsement, recommendation, or favoring by the United States Government or any agency thereof. The views and opinions of authors expressed herein do not necessarily state or reflect those of the United States Government or any agency thereof.

DISCLAIMER

Portions of this document may be illegible in electronic image products. Images are produced from the best available original document.

OXYGEN TRANSPORT IN THE $\text{Sr}_2\text{Fe}_{3-x}\text{Co}_x\text{O}_y$ SYSTEM

B. Ma,* U. Balachandran,* B.J. Mitchell,† J.W. Richardson, Jr.,† J.P. Hodges,‡ and J.D. Jorgensen†

*Energy Technology Division, Argonne National Laboratory, Argonne, IL 60439

†Intense Pulsed Neutron Source, Argonne National Laboratory, Argonne, IL 60439

‡Materials Science Division, Argonne National Laboratory, Argonne, IL 60439

ABSTRACT

The mixed-conducting Sr-Fe-Co oxide has potential use as a gas separation membrane. Its superior oxygen transport reveals the feasibility of using oxide membranes in large-scale oxygen separation. $\text{Sr}_2\text{Fe}_{3-x}\text{Co}_x\text{O}_y$ (with $x = 0.0, 0.3, 0.6,$ and 1.0) samples were made by solid state reaction. To understand the oxygen transport mechanism in this system, conductivity and thermogravimetry experiments were conducted at high temperature in various oxygen partial pressure environments. The oxygen diffusion coefficient was determined from the time relaxation transient behavior of the specimen after switching the surrounding atmosphere. Mobility of the charge carrier was derived from relative conductivity and weight changes. X-ray diffraction experiments were carried out on these samples to determine their crystal structures.

INTRODUCTION

Oxides with mixed electronic and oxygen ionic conductivities have been widely studied for use as components in high-temperature electrochemical devices such as solid-oxide fuel cells, oxygen sensors, oxygen pumps, batteries, and oxygen-permeable membrane catalysts [1-5]. The $\text{Sr}_2\text{Fe}_{3-x}\text{Co}_x\text{O}_y$ has not only high combined electronic and oxygen ionic conductivities but also appreciable oxygen permeability [6-8]. It holds particular promise as ceramic membranes designed to separate oxygen from air, being impervious to other gaseous constituents. $\text{Sr}_2\text{Fe}_2\text{CoO}_y$ can be used to produce syngas ($\text{CO} + \text{H}_2$) by direct conversion of methane and other basic hydrocarbon gases, such as coal gas, without external electrical circuitry [6]. The oxygen permeation flux through this type of membrane could be considered commercially feasible [9-12].

The intense interest in developing materials with high oxygen ionic conductivity has recently focused on perovskite and/or perovskite-related oxygen-deficient structures, for example, the brownmillerite structure [13]. Although the idealized perovskite structure does not contain oxygen vacancies, its structure is extremely versatile. Oxygen ionic conduction can be induced by incorporating oxygen vacancies into the structure. The brownmillerite structure is related to the perovskite structure but contains ordered oxygen vacancies that result in significant oxide ionic conduction (normally due to the existence of oxygen vacancies). In those materials, oxygen vacancies are the primary charge carriers for oxygen ionic conduction. Activation energies of these materials are normally greater than 1 eV, and the oxygen surface exchange rate is low. Unlike the brownmillerite and similar materials, $\text{Sr}_2\text{Fe}_{3-x}\text{Co}_x\text{O}_y$ utilizes interstitial oxide ions and holes as the predominant charge carriers in an oxygen-rich environment [7,14], and its oxygen surface exchange rate is sufficiently high that the oxygen transport is primarily bulk-controlled [15]. The oxygen ionic conductivity and oxygen permeability of $\text{Sr}_2\text{Fe}_{3-x}\text{Co}_x\text{O}_y$ are superior to these of other mixed-conducting materials. These unique transport properties make the $\text{Sr}_2\text{Fe}_{3-x}\text{Co}_x\text{O}_y$ a technologically important material.

In this paper, we focus on the relationships between structure and transport properties of the $\text{Sr}_2\text{Fe}_{3-x}\text{Co}_x\text{O}_y$ materials. We report X-ray powder diffraction results, temperature- and oxygen-partial-pressure ($p\text{O}_2$)-dependent electrical conductivity, mobility, and oxygen diffusion coefficient. Based on our experimental results, we attempt to build a coherent picture to correlate the structure, oxygen transport properties, and thermodynamics of the $\text{Sr}_2\text{Fe}_{3-x}\text{Co}_x\text{O}_y$ system.

EXPERIMENT

$\text{Sr}_2\text{Fe}_{3-x}\text{Co}_x\text{O}_y$ ($x = 0.0, 0.3, 0.6,$ and 1.0) powders were made by the solid-state reaction method. Details were reported earlier in Ref. 7. Pellets were made by pressing uniaxially with a 120-MPa load then sintering in air at $\approx 1200^\circ\text{C}$ for 5 h. The true density of $\text{Sr}_2\text{Fe}_{3-x}\text{Co}_x\text{O}_y$, measured on powder with AccuPyc 1330 pycnometry, agrees with the theoretical density obtained from the X-ray diffraction pattern. Bulk density of the sintered pellets was measured by the Archimedes method and found to be $\approx 95\%$ of the theoretical value. Scanning electron microscopy (SEM) and electron-dispersive X-ray (EDX) analysis revealed the good homogeneity and phase integrity of the sample.

X-ray powder diffraction analysis was carried out on a Scintag XDS-200 diffractometer. Data were taken by using $\text{Cu K}\alpha$ radiation. A high-purity intrinsic Ge energy-dispersive detector was used to minimize the backgrounds due to sample fluorescence. The diffraction data were analyzed with the Rietveld program [16].

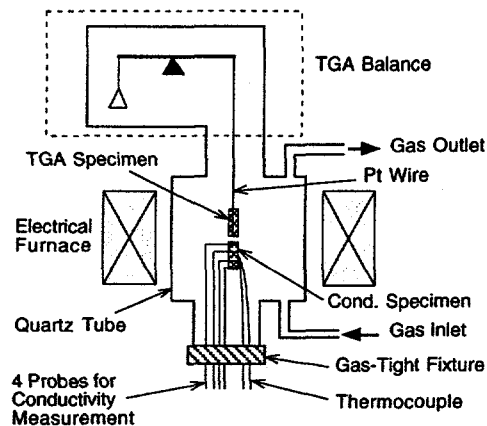


Fig. 1. Schematic drawing of experimental setup used for conductivity and thermogravimetric analysis.

Electrical conductivity of the $\text{Sr}_2\text{Fe}_{3-x}\text{Co}_x\text{O}_y$ sample was determined by the conventional four-probe method on bar specimens cut from the sintered pellets. Details of the experimental setup for high-temperature measurement were reported earlier [7]. Weight change of the specimen due to $p\text{O}_2$ change in the surrounding atmosphere was monitored and recorded by a CAHN TG-121 thermogravimetric analysis (TGA) apparatus. The atmosphere surrounding the specimen was controlled by using premixed gases of various $p\text{O}_2$ values. A schematic illustration of the experimental setup is shown in Fig. 1. To determine the oxygen diffusivity of $\text{Sr}_2\text{Fe}_{3-x}\text{Co}_x\text{O}_y$, we first equilibrated the specimen in an environment of specific $p\text{O}_2$ value, then abruptly changed the $p\text{O}_2$ in the surrounding atmosphere to a different value and monitored the weight change of the specimen as a function of time. The oxygen diffusion coefficient is thus determined from the time relaxation data [17]. Concentration change of oxide ions due to change of surrounding atmosphere is related to the weight change of the specimen. The change in concentration of oxide ions in the specimen is given by [18]

$$\Delta C_j = N_A \cdot \frac{\Delta W}{W} \cdot \frac{d}{M_o} \quad (1)$$

where ΔW and W are the weight change and the initial weight of the specimen, N_A is Avogadro's number ($6.022 \times 10^{23} \text{ mol}^{-1}$), d is the density of $\text{Sr}_2\text{Fe}_{3-x}\text{Co}_x\text{O}_y$, and M_o is the atomic weight of oxygen ($16 \text{ g}\cdot\text{mol}^{-1}$). Conductivity is related to the concentration of j th charge carriers by

$$\sigma_j = C_j Z_j e \mu_j \quad (2)$$

where C_j is the number density of charge carriers of type j (in cm^{-3}), Z_j is the number of the electron charge carried by these carriers, e is the elementary electron charge (in C), and μ_j is the mobility of the j th charge carriers in the solid (in $\Omega\cdot\text{cm}^2\cdot\text{V}^{-1}$). Substituting Eq. 1 into Eq. 2, we can then express the mobility of oxide ions as

$$\mu_o = \frac{8}{F} \cdot \frac{W}{d} \cdot \frac{\Delta\sigma}{\Delta W} \quad (3)$$

where F is the Faraday constant, and $Z_j = 2$ for oxide ions.

The oxygen chemical diffusion coefficient of $\text{Sr}_2\text{Fe}_2\text{CoO}_y$ measured by the conductivity relaxation method was reported earlier [17]. During the weight relaxation experiments, we abruptly changed the $p\text{O}_2$ in the surrounding atmosphere and then monitored specimen weight change by using TGA as a function of time. The diffusion process of the oxygen ions is described by Fick's second law:

$$\frac{\partial C}{\partial t} = \text{div}(D \cdot \text{grad } C) \quad (4)$$

where D is the oxygen chemical diffusion coefficient (in $\text{cm}^2 \cdot \text{sec}^{-1}$), and C is the concentration of the diffusing substance.

The transient behavior in the reequilibration process was analyzed by fitting the time relaxation data to the solution of Fick's second law with appropriate boundary conditions. For a thin slab specimen, weight change during the relaxation process can be expressed by [18]

$$\frac{W(t) - W(0)}{W(\infty) - W(0)} = 1 - \sum_{n=0}^{\infty} \frac{8}{(2n+1)^2 \pi^2} \exp\left(-\frac{(2n+1)^2 \pi^2 D t}{4l^2}\right) \quad (5)$$

where l is the half-thickness of the specimen slab (in cm), and $W(t)$, $W(0)$, $W(\infty)$ are the weights of specimen at time t , at the starting time, and at infinite time. The oxygen diffusion coefficient can be determined by least-squares fitting of the time-dependent weight relaxation data, $W(t)$, to Eq. 5.

RESULTS AND DISCUSSION

X-ray diffraction profiles of the sintered $\text{Sr}_2\text{Fe}_{3-x}\text{Co}_x\text{O}_y$ and, for comparison, $\text{SrFe}_{0.8}\text{Co}_{0.2}\text{O}_{3-\delta}$ perovskite are plotted in Fig. 2. Rietveld profile analysis of the diffraction data was performed to determine the phase composition of the synthesized samples. For the $\text{Sr}_2\text{Fe}_3\text{O}_y$ sample ($x = 0$) a satisfactory fit to the diffraction profile was obtained (see Fig. 3) using for initial atom positions a crystallographic model of $\text{Sr}_4\text{Fe}_6\text{O}_{13}$ as reported by Yoshiasa et al. [19]. No evidence of secondary phases was found in sample $\text{Sr}_2\text{Fe}_3\text{O}_y$, indicating that it was phase-pure. The crystal structure of $\text{Sr}_2\text{Fe}_3\text{O}_y$ is particularly interesting because Fe^{3+} cations are present with three

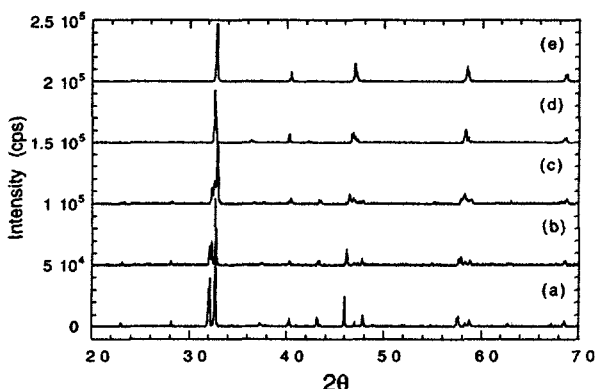


Fig. 2. Room-temperature X-ray diffraction profiles of air-sintered samples: (a) $\text{Sr}_2\text{Fe}_3\text{O}_y$, (b) $\text{Sr}_2\text{Fe}_{2.4}\text{Co}_{0.6}\text{O}_y$, (c) $\text{Sr}_2\text{Fe}_2\text{CoO}_y$, (d) $\text{Sr}_2\text{Fe}_{1.6}\text{Co}_{1.4}\text{O}_y$, and (e) $\text{SrFe}_{0.8}\text{Co}_{0.2}\text{O}_{3-\delta}$.

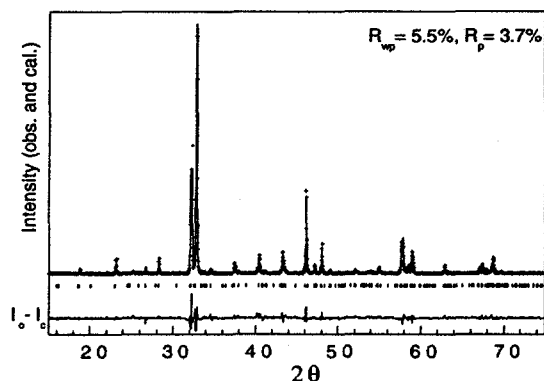


Fig. 3. Rietveld profile fit to powder X-ray diffraction data of $\text{Sr}_2\text{Fe}_3\text{O}_y$ sample. Observed, calculated, and difference profiles are shown along with reflection markers.

different oxygen coordinations: octahedral, trigonal-bipyramidal and square-pyramidal. The structure is also layered and can be thought of as consisting of alternating SrFeO_3 and Fe_2O_3 blocks. A schematic representation of the $\text{Sr}_4\text{Fe}_6\text{O}_{13}$ crystal structure is shown in Fig. 4.

Table 1. Phase compositions of air-sintered $\text{Sr}_2\text{Fe}_{3-x}\text{Co}_x\text{O}_y$ samples and unit cell parameters of component phase.

x	$\text{Sr}_2\text{Fe}_{3-x}\text{Co}_x\text{O}_y$	$\text{SrFe}_{1-z}\text{Co}_z\text{O}_{3-\delta}$	CoO	a (Å)	b (Å)	c (Å)	V (Å ³)
0.0	> 98%	-	-	11.126	18.978	5.5864	1179.6
0.3	≈ 95%	≈ 4%	≈ 1%	11.085	19.016	5.5670	1173.5
0.6	≈ 90%	≈ 8%	≈ 2%	11.065	19.008	5.5618	1169.8
1.0	≈ 70%	≈ 25%	≈ 5%	11.017	19.030	5.5463	1162.8

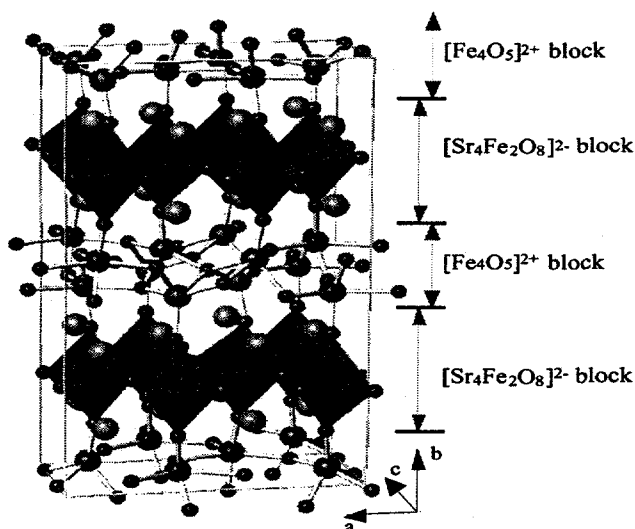


Fig. 4. Schematic representation of $\text{Sr}_4\text{Fe}_6\text{O}_{13}$ crystal structure.

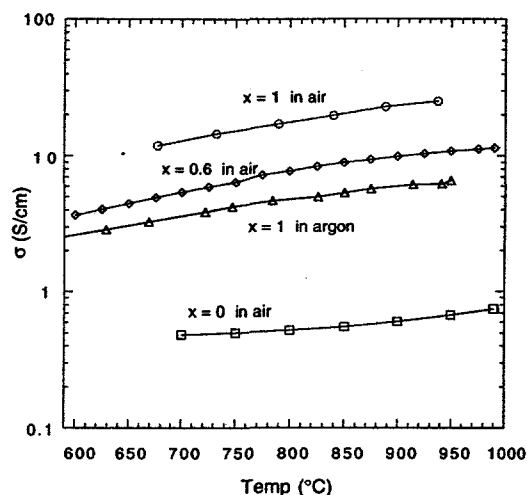


Fig. 5. Conductivity of $\text{Sr}_2\text{Fe}_{3-x}\text{Co}_x\text{O}_y$ samples plotted as a function of temperature.

For the $\text{Sr}_2\text{Fe}_2\text{CoO}_y$ sample ($x = 1$), however, Rietveld analysis revealed a multiphase composition of ≈70% weight fraction (wtf) $\text{Sr}_2\text{Fe}_{3-x}\text{Co}_x\text{O}_y$ ($x \approx 1$), 25% wtf $\text{SrFe}_{1-z}\text{Co}_z\text{O}_{3-\delta}$ ($z \approx 0.33$) and 5% wtf CoO. The lower cobalt substituted samples, with $x = 0.3$ and 0.6, were composed of ≈90% wtf of the layered $\text{Sr}_2\text{Fe}_{3-x}\text{Co}_x\text{O}_y$ phase and minor amounts of perovskite $\text{SrFe}_{1-z}\text{Co}_z\text{O}_{3-\delta}$ and CoO. Incorporation of cobalt into the structure of $\text{Sr}_2\text{Fe}_{3-x}\text{Co}_x\text{O}_y$ leads to a steady change in unit cell parameters with increasing cobalt doping, x , as shown in Table 1. The $\text{Sr}_2\text{Fe}_{3-x}\text{Co}_x\text{O}_y$ unit cell volume gradually decreases with increasing cobalt substitution, as expected, because the ionic radius of Co^{3+} cation, $r_i(\text{VI}) = 0.61 \text{ \AA}$ is less than $r_i(\text{VI}) = 0.645 \text{ \AA}$ of the Fe^{3+} cation.

Table 2. Equilibrium conductivities and weights of a $\text{Sr}_2\text{Fe}_2\text{CoO}_y$ specimen in various oxygen partial pressure environments at 950°C

Atmosphere	$\log(p\text{O}_2)$	M (mg)	σ (S/cm)
100% O_2	0	155.1365	25.17
air	-0.678	154.9001	22.68
0.4% O_2	-2.373	154.7498	20.26
1% CO/CO_2	-11.5	153.0345	1.13
8% $\text{H}_2/\text{H}_2\text{O}$	-18.2	144.8230	0.94

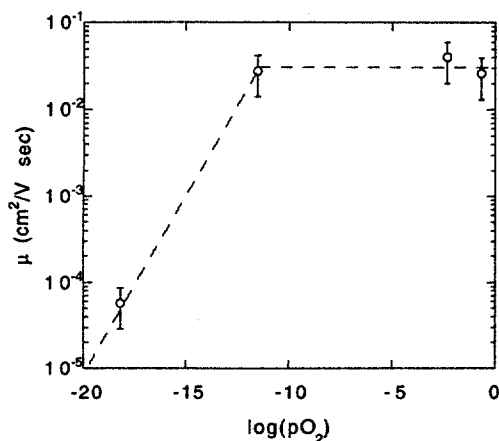


Fig. 6. Mobility of $\text{Sr}_2\text{Fe}_2\text{CoO}_y$ as a function of oxygen partial pressure.

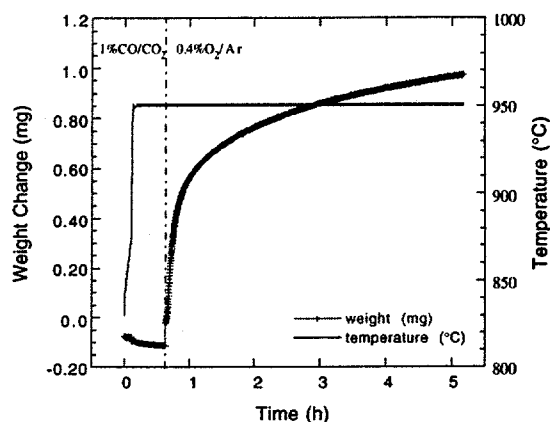


Fig. 7. Weight change of $\text{Sr}_2\text{Fe}_2\text{CoO}_y$ as a function of time after switching surrounding atmosphere from 1% CO/CO_2 to 0.4% O_2/Ar .

The conductivity of $\text{Sr}_2\text{Fe}_{3-x}\text{Co}_x\text{O}_y$ increases with increasing x , as shown in Fig. 5. The equilibrium conductivities and weights of $\text{Sr}_2\text{Fe}_2\text{CoO}_y$ in various environments at 950°C are listed in Table 2. Conductivity increases with increasing $p\text{O}_2$. The mobility of oxide ions in $\text{Sr}_2\text{Fe}_2\text{CoO}_y$ can be estimated by substituting the data into Eq. 3, and the result is plotted in Fig. 6. At high $p\text{O}_2$, mobility is almost independent of $p\text{O}_2$ and has a value of $\approx 3 \times 10^{-2} \text{ cm}^2 \cdot \text{V}^{-1} \cdot \text{sec}^{-1}$. At low $p\text{O}_2$, however, mobility is lower by more than two orders of magnitude. This may imply that the interaction between oxide ions and their sublattices is stronger at low $p\text{O}_2$, and that the interaction becomes steadily weaker with increasing $p\text{O}_2$. When $p\text{O}_2$ is greater than a certain value, the interaction tends to be saturated and to become independent of $p\text{O}_2$.

Table 3. Oxygen diffusion coefficient of $\text{Sr}_2\text{Fe}_2\text{CoO}_y$ in various $p\text{O}_2$ environments at 950°C

Atmosphere Change	$\Delta \log(p\text{O}_2)$	$D (\text{cm}^2 \cdot \text{sec}^{-1})$
100% O_2 to Air	-0.678	5.27×10^{-7}
Air to 0.4% O_2/Ar	-1.695	7.13×10^{-7}
0.4% O_2/Ar to Air	+1.695	5.38×10^{-6}
0.4% O_2/Ar to 1% CO/CO_2	-9.127	1.36×10^{-6}
1% CO/CO_2 to 0.4% O_2/Ar	+9.127	1.68×10^{-6}
1% CO/CO_2 to 8% $\text{H}_2/\text{H}_2\text{O}$	-6.700	7.18×10^{-7}

Figure 7 shows a typical example of the weight change of $\text{Sr}_2\text{Fe}_2\text{CoO}_y$ as a function of time after switching the surrounding atmosphere. Relaxation data were analyzed by a least-squares fitting to Eq. 5 with geometry parameters of the specimen. Experimental data and their fittings are shown in Fig. 8. Agreement appears to be good between the experimental data and the fitting curve. Oxygen diffusion coefficients of $\text{Sr}_2\text{Fe}_2\text{CoO}_y$ at 950°C in various $p\text{O}_2$ environments are given in Table 3. The oxygen chemical diffusion coefficient of $\text{Sr}_2\text{Fe}_{3-x}\text{Co}_x\text{O}_y$ is $\approx 10^{-6} \text{ cm}^2 \cdot \text{sec}^{-1}$ at 950°C .

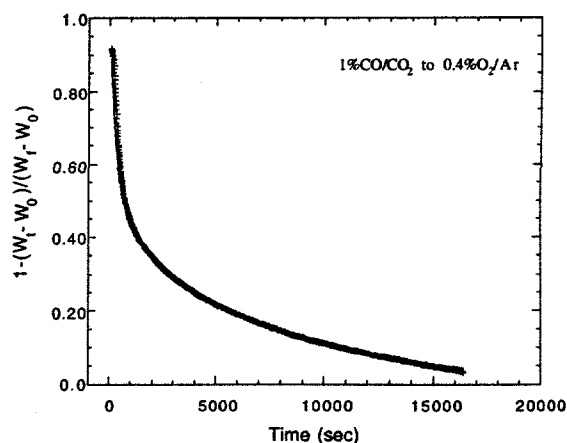


Fig. 8. Time relaxation data and its theoretical fitting for $\text{Sr}_2\text{Fe}_2\text{CoO}_y$.

CONCLUSIONS

The phase composition of the $\text{Sr}_2\text{Fe}_{3-x}\text{Co}_x\text{O}_y$ samples was found to be strongly dependent on cobalt content. The $\text{Sr}_2\text{Fe}_3\text{O}_y$ sample is a single-phase material, whereas the cobalt-containing samples are multiphase. The amount of $\text{SrFe}_{1-z}\text{Co}_z\text{O}_{3.8}$ perovskite phase in the cobalt-containing samples increases disproportionately with x . Conductivity of $\text{Sr}_2\text{Fe}_{3-x}\text{Co}_x\text{O}_y$ increases with increasing cobalt content and increasing $p\text{O}_2$. At 950°C in air, the conductivity of $\text{Sr}_2\text{Fe}_2\text{CoO}_y$ is $\approx 25 \text{ S}\cdot\text{cm}^{-1}$. At high $p\text{O}_2$, mobility is almost independent of $p\text{O}_2$ and has a value of $\approx 3 \times 10^{-2} \text{ cm}^2\cdot\text{V}^{-1}\cdot\text{sec}^{-1}$. At low $p\text{O}_2$, however, mobility is lower by more than two orders of magnitude. The oxygen chemical diffusion coefficient of $\text{Sr}_2\text{Fe}_{3-x}\text{Co}_x\text{O}_y$ is $\approx 10^{-6} \text{ cm}^2\cdot\text{sec}^{-1}$ at 950°C .

ACKNOWLEDGMENT

Work at Argonne National Laboratory is supported by the U.S. Department of Energy, Federal Energy Technology Center, under Contract W-31-109-Eng-38.

REFERENCES

1. T. Takahashi and H. Iwahara, *Energy Convers.*, **11**, 105 (1971).
2. B.C.H. Steele, *Mater. Sci. Eng. B-Solid State M.*, **13**, 79 (1992).
3. N.Q. Minh, *J. Am. Ceram. Soc.*, **76**, 563 (1993).
4. R. DiCosimo, J.D. Burrington, and R.K. Grasselli, *J. Catal.*, **102**, 377 (1992).
5. K.R. Kendall, C. Navas, J.K. Thomas, and H.-C. Loye, *Solid State Ionics*, **82**, 215 (1995).
6. U. Balachandran, T.J. Dusek, S.M. Sweeney, R.B. Poeppel, R.L. Mieville, P.S. Maiya, M.S. Kleefisch, S. Pei, T.P. Kobylinski, C.A. Udovich, and A.C. Bose, *Am. Ceram. Soc. Bull.*, **74**, 71 (1995).
7. B. Ma, J.-H. Park, C.U. Segre, and U. Balachandran, *Mater. Res. Soc. Symp. Proc.*, **393**, 49 (1995).
8. H. Deng, M. Zhou, and B. Abeles, *Solid State Ionics*, **74**, 75 (1994).
9. S. Pei, M.S. Kleefisch, T.P. Kobylinski, J. Faber, C.A. Udovich, V. Zhang-McCoy, B. Dabrowski, U. Balachandran, R.L. Mieville, and R.B. Poeppel, *Catal. Lett.*, **30**, 201 (1995).
10. T.J. Mazanec, T.L. Cable, and J.G. Frye, Jr., *Solid State Ionics*, **53-56**, 111 (1992).
11. T.L. Cable, European Patent EP 0438 902 A2, July 31 (1991).
12. Y. Teraoka, T. Nobunaga, and N. Yamazoe, *Chem. Lett.*, **1988**, 503 (1988).
13. M.T. Anderson, J.T. Vaughey, and K.R. Poeppelmeier, *Chem. Mater.*, **5**, 151 (1993).
14. B. Ma, U. Balachandran, J.-H. Park, and C.U. Segre, *J. Electrochem. Soc.*, **143**, 1736 (1996).
15. B. Ma, J.P. Hodges, J.D. Jorgensen, D.J. Miller, J.W. Richardson, Jr., and U. Balachandran, to be published in *J. Solid State Chem.*, (1999).
16. H.M. Rietveld, *J. Appl. Cryst.*, **2**, 65 (1969).
17. B. Ma, U. Balachandran, J.-H. Park, and C.U. Segre, *Solid State Ionics*, **83**, 65 (1996).
18. B. Ma, U. Balachandran, *Solid State Ionics*, **100**, 53 (1997).
19. A. Yoshiasa, K. Ueno, F. Kanamaru, and H. Horiuchi, *Mater. Res. Bull.*, **21**, 175 (1986).